

Influence of Subducting Topography on Earthquake Rupture

■ Susan L. Bilek

Abstract

Rupture models for large subduction zone earthquakes suggest significant heterogeneity in slip and moment release over the fault plane. Attempts to characterize the nature of the high-slip regions led to descriptions of these earthquakes in the context of the asperity model and allowed for subduction zones to be classified on the basis of likely earthquake asperity distributions. Understanding the physical features in the fault zone that produce these high-slip regions is still a challenge. Detailed bathymetric and seismic data collection in several subduction zones has led to correlations between large earthquake rupture patterns and subducting features such as seamounts and ridges. This is not a simple relationship, and it is not consistent in all subduction zones. Earthquakes at several subduction zones appear to concentrate slip on subducted features, but others have features that act as barriers to earthquake rupture. Additional questions remain about the temporal stability of high-slip regions. More research is needed to understand the connections between the upper plate, fault friction, subducting features, and overall subduction zone stresses and the patterns of large earthquakes in this complex environment.

Earthquake Slip and Asperities

Early definitions of asperities go back to Amonton, who proposed that static friction on a fault relates to the overall roughness of the fault surface. Increased roughness on the surface may be caused by increased occurrence of protrusions on the surface. He defined asperities as welded contacts along the fault. Early asperity models for earthquakes were developed using results from laboratory rock friction experiments [Byerlee, 1967; Scholz and Engelder, 1976].

These models suggest that faults are held together by high strength contacts, or Amonton's asperities. Stresses at the asperities were typically higher than at other portions of the fault. The physical causes of asperities along faults were related to variations in geometry, friction, or material properties along the fault.

Understanding the relationship between earthquakes and asperities advanced with increased analysis of higher-quality seismic data. Earthquake seismograms from a global distribution of seismic stations were used to examine the seismic moment release distribution and slip during large earthquakes. Many of these observations for continental and subduction zone earthquakes show high moment release, high slip, occurring in distinct patches on the fault plane rather than smoothly varying over the fault plane [Wyss and Brune, 1967; Trifunac and Brune, 1970; Kanamori, 1978; Ruff and Kanamori, 1983; Schwartz and Ruff, 1987; Mendoza and Hartzell, 1988; Heaton, 1990; Wald et al., 1991; Wald and Heaton, 1994; Ma et al., 2001; Ji et al., 2002] (fig. 5.1).

High-slip patches can be converted to relatively high stress drops, suggesting that these patches are areas of increased strength compared to the surrounding regions and can be considered asperities.

Small-magnitude earthquakes have also been used to describe asperity distribution on faults. Nadeau and Johnson [1998] suggest clustering of microearthquakes along the Parkfield segment of the San Andreas fault indicates asperity locations. They suggest that the earthquake clusters define high-strength patches able to break within weaker zones along the fault, although the high-stress drop values calculated for these earthquakes appear to be higher than

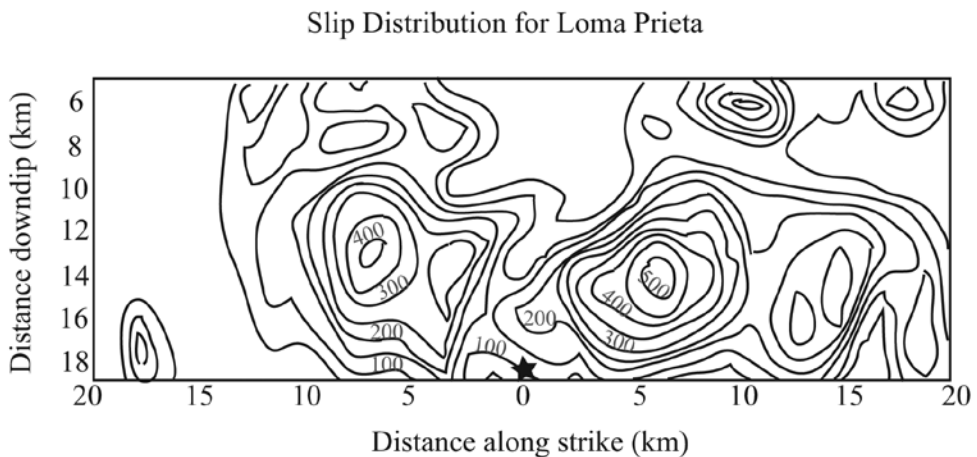


Figure 5.1 Slip distribution for the 1989 Loma Prieta earthquake, modified from Beroza [1991], with contours of slip in centimeters. A clear pattern of heterogeneous slip is observed for this continental earthquake, with two significant patches of high slip (asperities). Other models of strong motion and teleseismic data show consistent features [e.g., Wald et al., 1991].

estimates from other small earthquakes [Sammis and Rice, 2001]. Detailed locations of small earthquakes in subduction zones have also yielded observations of clusters and suggestions of heterogeneous asperity distribution along these faults [e.g., Hino et al., 1996; Matsuzawa et al., 2002; Igarashi et al., 2003; Obana et al., 2003; DeShon et al., 2003].

Seismic Observations of Heterogeneity

Several observations are used to suggest heterogeneity in earthquake rupture. Locations and recurrence patterns of large and small earthquakes as well as aftershock patterns provide some indication of heterogeneity levels on faults. Additionally, analysis of seismic waveforms yields source time functions that describe the time history of seismic moment release.

Earthquake Locations

Earthquake location and recurrence patterns provide estimates of heterogeneity. Along the Nankai margin, large events ($M \sim 8$) appear to break similar zones over time in fairly regular patterns [Ando, 1975], suggesting some level of segmentation or high-strength zones that persist over a few earthquake cycles. To the north in the Japan Trench, large earthquake locations are less regular. The occurrence of doublets, similar magnitude large earthquakes that occur in pairs with small spatial and temporal separation, also have implications for distribution of high-strength zones. They appear to be a failure at one asperity, triggering failure at an adjacent asperity [Lay and Kanamori, 1980; Xu and Schwartz, 1993]. Additionally, locations of small earthquakes and microseismicity have also been used to map out zones of strength heterogeneity along faults.

Source Time Functions

The source time function provides the seismic moment release history for the earthquake. An earthquake with a smooth rupture is best modeled with a trapezoid-like shape source time function, implying smooth average slip over the entire fault plane. However, source time functions from most earthquakes are not trapezoidal because slip does not occur smoothly over the fault area (e.g., fig. 5.1).

In order to obtain estimates of earthquake source time functions, seismologists model seismic waveforms, deconvolving estimates of Earth structure effects on wave propagation from the source time function [e.g., Kikuchi and Kanamori, 1986; Ammon et al., 1993]. This modeling provides estimates for the locations of moment release on the fault plane as well as the time history of moment release. Because seismic moment is related to fault area and earthquake slip, the slip distribution along the fault can also be determined.

Models for Subduction Zone Earthquakes

Because most of the world's largest earthquakes occur in the shallow subduction zone, significant data exist about earthquake rupture patterns in this tectonic environment. Many observations of complex waveforms and source time functions for subduction zone earthquakes were used to formulate asperity models in the 1970s and 1980s specifically for subduction zone environments. *Kanamori [1978]* suggested that small subduction zone earthquakes result from rupture at a single asperity; complex multiple earthquakes or doublets can result when asperity failure induces large stresses on adjacent asperities to generate multiple failures. *Lay et al. [1982]* use a variety of observations to characterize the relative distribution of asperities in subduction zones and connect this distribution to great subduction zone earthquakes. By summarizing rupture process observations or many large earthquakes, such as location, aftershock distributions, and source time function shapes, they relate rupture patterns to features in trench morphology. Observations of time function variations and complex waveforms suggest that high-frequency seismic body waves are radiated from small parts of the rupture plane, the asperities or strong patches of the fault. Low-frequency seismic radiation and aftershocks originate from the rest of the rupture area described as a weak zone relative to the asperities. Within this model, more complicated ruptures suggest smaller and more heterogeneously distributed strong patches on the fault.

AU: In the following statement, “on” meant instead of “or”? “By summarizing rupture process observations or many large earthquakes...”

Using the foundations of the asperity model, *Lay et al. [1982]* divide subduction zones into several classes, roughly on the basis of the rupture length of large and great earthquakes and thus asperity distribution. Each class is used to characterize the expected regional stress conditions and seismic coupling (fig. 5.2). A Chile-type margin, characterized by great earthquakes with rupture lengths of over 500 km, describes the Chile, Alaska, and Kamchatka subduction zones. These great earthquakes tend to repeat at nearly identical locations. Large sections of the margin typically have few large subducting features such as seamounts or ridges, allowing for fairly smooth contact between the subducting and overriding plates. Representative earthquakes for the margins in this class (group I), such as the $M_w = 9.5$ 1960 Chile and the $M_w = 9.2$ 1964 Alaska, have very long duration and relatively simple source time functions, suggesting that these margins are strongly coupled with smooth plate contacts and almost uniform asperity distribution.

Subduction zones characterized by large earthquakes with rupture lengths of up to 500 km fall into the next class of margins (group II). These regions, such as the western Aleutians, Nankai, and Colombia, have variations in earthquake rupture patterns, with occasional earthquakes rupturing over several sections of the margin and others breaking only single segments. Source time functions for earthquakes at these margins typically have more complexity than those from the Chile-type margins. These regions have been described as having large asperities, although not as large as in the

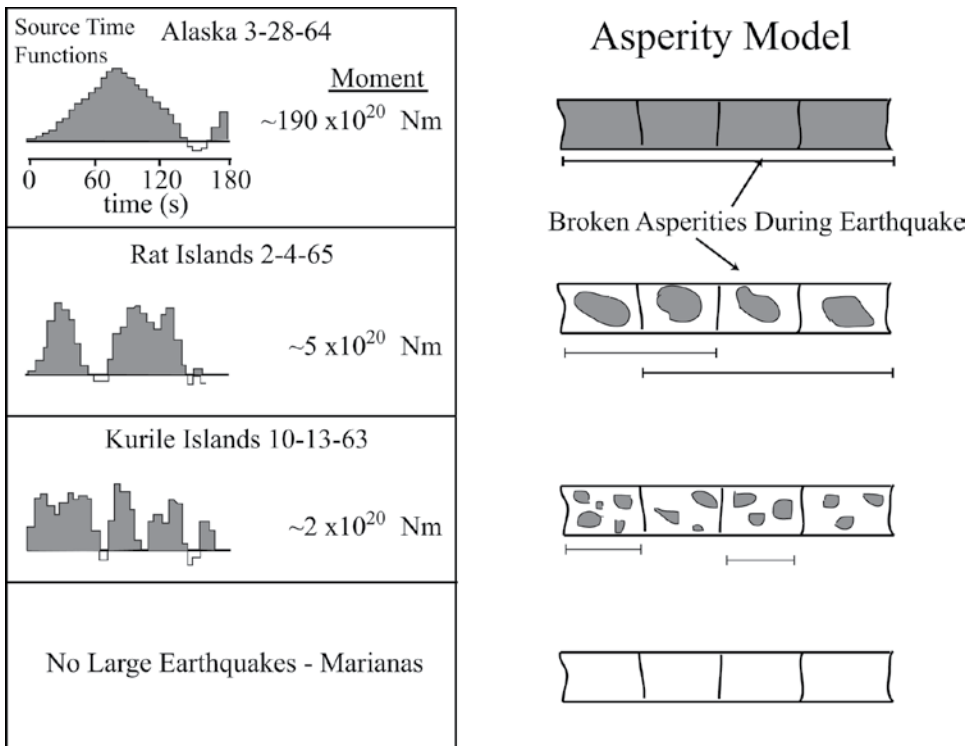


Figure 5.2 The asperity model for subduction zone earthquakes, modified from *Ruff and Kanamori* [1980] and *Lay et al.* [1982]. (left) An example source time functions (moment release during earthquake rupture), for representative earthquakes in each of the main asperity classes (right). The great 1964 Alaska earthquake had a fairly simple source time function, suggesting little heterogeneity in body-wave radiation and slip distribution along the fault plane. The corresponding asperity distribution for this earthquake (as well as the 1960 Chile earthquake) is a very large, mostly continuous strong fault area, shown in green. Large earthquakes farther along the Aleutians also have large strong patches of fault area, but somewhat smaller than the 1960 Chile or 1964 Alaska case. Source time functions for earthquakes in the Aleutians (and regions such as Nankai and Colombia) have a few large pulses of moment release, reflecting the change in asperity distribution on the fault plane. Regions such as the Kuriles, Peru, and Central America make up the next class of margin, with a very heterogeneous asperity pattern on the fault plane. These earthquakes have significantly more complex source time functions, representing the rupture of multiple small asperities on the fault. The final class of margin includes the Marianas and Izu-Bonin arcs, regions which do not produce great earthquakes because of the lack of large strong patches on the subduction megathrust.

AU: Figure 5.2 caption mentions color. File provided in black and white.

Chile-type margin. Rupture of one asperity may cause stress changes large enough to cause other large asperities to fail, as suggested by *Ruff* [1992], although this may depend on the relative size and separation of these large asperities.

The next group of margins (group III) shows increased complexity, as the Kurile Islands, Peru, central Chile, and Japan subduction zones typically have large earthquakes with rupture zones of ~100–300 km in length. These earthquakes, which tend to repeat in similar locations, typically do not grow into great earthquakes by breaking other segments. Earthquakes in these regions typically produce complex body waves, leading to more complex source time functions. Asperities for these regions tend to vary in size but are typically smaller than expected for the Aleutian (group II) type. Because of the smaller and more heterogeneous asperity size distribution, these earthquakes rarely rupture continuous sections of the margin as seen in the Chile-type margins (group I). An intermediate subgroup includes margins such as New Hebrides and Middle America, which have earthquakes with rupture lengths of 100–150 km and tend to produce fairly simple body waves and source time functions. These margins may have smaller asperities and larger separations between them, making it less likely that an earthquake could rupture more than one asperity.

Subduction zones such as Marianas, Izu-Bonin, and Ryukyu make up the final group (IV) in the asperity model. Great or very large earthquakes are rare in these subduction zones, suggesting that there is a lack of asperities large enough to produce these earthquakes. Small earthquakes and repeating clusters of small earthquakes may occur, but because the *Lay et al.* [1982] study focused only on large and great earthquakes, these margins were classified as relatively aseismic because of the lack of large and great earthquakes.

Physical Nature of Asperities

Using the asperity model framework, regional variations in subduction zone earthquake rupture patterns are ascribed to a distribution of variously sized asperities. Although an asperity is defined as a region of increased strength on the fault plane and location of high slip during an earthquake [e.g., *Byerlee*, 1967; *Lay et al.*, 1982; *Kanamori*, 1986], the question of what can make an asperity is more complicated. Reviewed below are several possibilities for increasing fault zone strength, including an influence from the upper plate, frictional variations within the fault zone, and specific features with high or variable relief on the subducting plate.

Upper Plate Strength

Variability in fore-arc conditions may impact strength on the subduction interface. *McCaffrey* [1993, 1994] suggests changes in fore-arc rheology controls the locations of great earthquakes. By classifying fore-arc strength using deviations between slip vectors and the plate convergence directions, *McCaffrey* [1993, 1994] finds that great megathrust earthquakes occur in regions where

fore arcs are more rigid (i.e., only small deviation between slip and convergence directions).

Beck and Christensen [1991] tie heterogeneous slip during the 1965 $M_w = 8.7$ Rat Islands earthquake to segmentation in the Aleutian fore arc. The fore arc contains fault controlled canyons and basins that separate distinct blocks of undeformed material. High moment release occurred near the centers of the undeformed blocks, but little moment release was observed at the edges of the blocks. *Ryan and Scholl* [1993] support these conclusions with additional data from other large earthquakes and aftershock locations, suggesting that the strong fore-arc blocks dictate asperity locations on the deeper interface in the Aleutians.

Friction Variations

In addition to plate strength, variations in friction along the fault plane likely influence slip during earthquakes. Using numerical simulations of earthquake slip, *Rice* [1993] suggests that high-slip patches may be controlled by frictional characteristics on a fault plane. Within subduction zones, *Song and Simons* [2003] correlate strong negative trench parallel gravity anomalies with slip in large and great earthquakes. They relate the observed negative gravity variations to high-shear traction on the interplate thrust. The negative anomalies observed in the zones of great earthquake slip suggest a reduction in normal stress, which tends to reduce stick-slip behavior. *Song and Simons* [2003] suggest an increase in the effective coefficient of friction to offset the decrease in normal stress, producing high-shear stresses along the fault.

Subducting Plate Features

In their discussion of the asperity model, *Lay et al.* [1982] suggest seafloor features can dictate asperity size in subduction zones. Specifically, large segments of smooth plate, possibly in the presence of subducted sediment, can provide large strong regions on the thrust interface [*Hilde*, 1983; *Ruff*, 1989]. Additionally, there appears to be a positive correlation between the occurrence of great earthquakes and the amount of sediment near the trench [*Ruff*, 1989]. However, detailed slip patterns of large and great earthquakes have not been compared with detailed maps of sediment distribution along these margins.

Features that produce roughness or topography on the subducting plate are also suggested to influence earthquake slip distributions. Horst and graben structures provide a rough plate interface with alternating strong and weak contact zones with the overriding plate [*Tanioka et al.*, 1997]. Other subducted high-relief features, such as fracture zones, seamounts, and ridges, also make likely candidates to influence earthquake behavior, as these topographic highs could cause isolated strong coupling with the overriding plate [e.g., *Kelleher and McCann*, 1976, 1977; *Cloos*, 1992; *Cloos and Shreve*, 1996;

Scholz and Small, 1997]. There have been several correlations between subducting features and specific earthquakes within several subduction zones, as described below.

Examples of Subducting Features and Large Earthquake Occurrence

In recent years, there have been significant strides toward the identification of features on the subducting plate before and after it enters the trench using high-quality bathymetry and seismic data. In several subduction zones, large earthquakes have occurred that may be related to these subducting features, suggesting that bathymetric features such as seamounts and ridges may act as regions of high stress and high seismic coupling, providing a physical link to asperity distributions.

NE Japan

Seamounts have been imaged near the trench along the northeastern margin of Japan [Lallemand and Pichon, 1987; Lallemand et al., 1989]. In addition, variation in subducting plate roughness, from smooth segments to portions featuring several horst and graben structures, has been mapped using bathymetry data. These features may impact the size and types of earthquakes possible along the margin, as suggested by Tanioka et al. [1997]. In regions of smooth, sedimented seafloor to the northern part of Honshu, large underthrust earthquakes such as the 1968 $M_w = 8.2$ Tokachi-Oki and 1994 $M_w = 7.7$ Sanriku events are typical. In regions of rough plate subducting, smaller earthquakes occur, along with more unusual events such as the 1896 tsunami earthquake.

Java

Within the Java subduction zone, sonar data show seamounts on the incoming plate as well as entering the subduction zone at the Java trench [Masson et al., 1990]. A $M_w = 7.8$ earthquake in 1994 occurred in this region, with principal slip located primarily in the region of a previously identified subducted seamount [Abercrombie et al., 2001] (fig. 5.3). In general, this subduction zone does not produce many large underthrusting events, so Abercrombie et al. [2001] suggest that most of the Java subduction zone is weakly coupled except in the areas of subducted seamounts. These seamounts provide higher coupling with the overriding plate and are locations for the large earthquakes and high slip in this region.

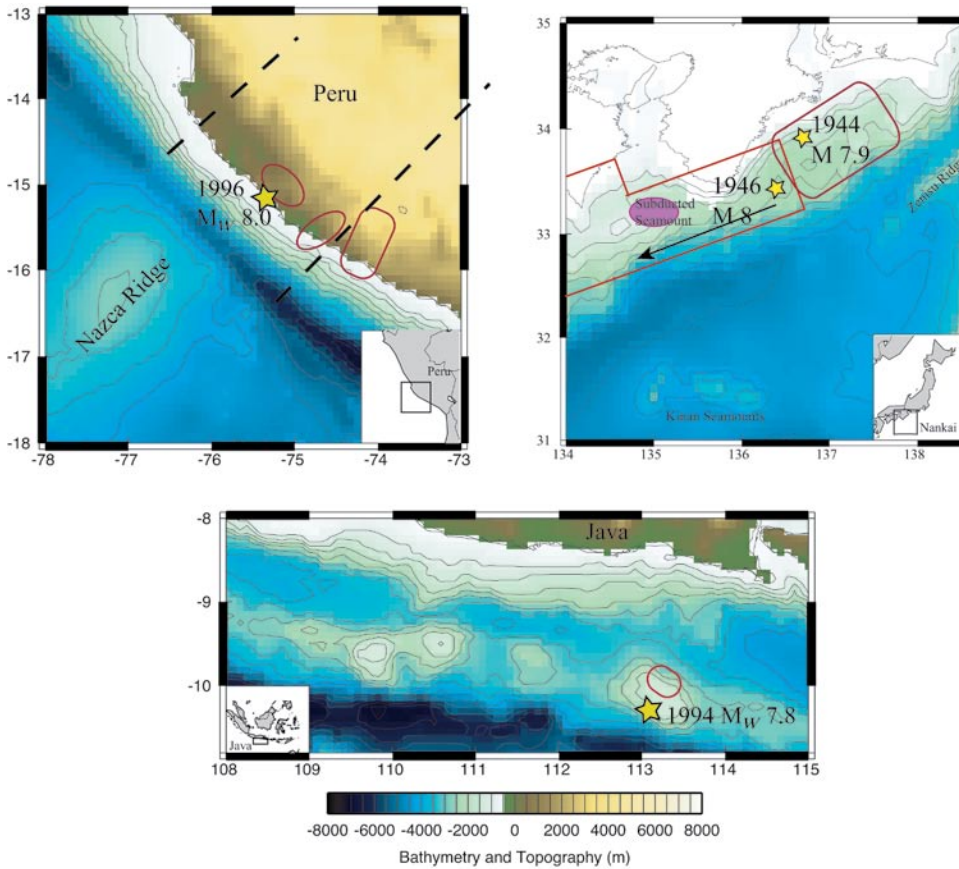


Figure 5.3 Examples of documented earthquake slip distributions impacted by subducting features. Bathymetry data are from the National Geophysical Data Center (<http://www.ndgc.noaa.gov/mgg/bathymetry>). The 1996 underthrust earthquake (star represents epicenter) in Peru had high slip (patches outlined in red) in the region of Nazca Ridge subduction as well as along the southern flank of the ridge [Spence *et al.*, 1999]. The dashed lines represent the likely location of previously subducted Nazca Ridge [Spence *et al.*, 1999]. Along the Nankai Trough, previously subducted seamounts (purple) and ridges have been imaged in the areas of the 1944 and 1946 great earthquakes. Kodaira *et al.* [2000] suggests that main seismogenic rupture for the 1946 propagated westward from the epicenter, stopping at the subducted seamount, with slow tsunamigenic slip southwest of the seamount. Using the pattern of the high slip for the 1994 earthquake, Kodaira *et al.* [2003] suggests a previously subducted Zenisu Ridge type feature prevented further NE directed rupture from the 1944 great earthquake. Along the Java subduction zone (bottom), Abercrombie *et al.* [2001] find high slip for the 1994 underthrust earthquake, one of the few large underthrust earthquakes in this region, collocated with a previously subducted seamount, as defined by the high spot in the bathymetry data.

Alaska-Aleutians

Bathymetry data from the eastern Aleutians show several seamount groups seaward of the Alaska-Aleutian Trench [Estabrook *et al.*, 1994]. Previously subducted seamounts, similar to the seamount groups currently observed such as the Gulf of Alaska seamounts, may be responsible for several earthquakes of $M \sim 7$ that repeat with almost identical depths, source radii, and focal mechanisms [Estabrook *et al.*, 1994]. Within the western Aleutians, earthquake catalogs do not contain many of these repeating-type earthquakes with similar source parameters, and corresponding bathymetry data do not show many seamounts on the subducting plate in this area.

Tonga

Seamounts in the Tonga-Kermadec subduction zone have been observed in satellite gravity data as well as bathymetry surveys [Balance *et al.*, 1989; Chapel and Small, 1996]. Within the Tonga Trench, several of these seamounts also correspond with locations of large underthrusting earthquakes. An $M_w \sim 8.0$ earthquake occurred in 1919 in the region of the Capricorn seamounts [Pacheco and Sykes, 1992]. In the region of the subducting Louisville Ridge, an $M_w = 7.5$ earthquake occurred in 1982 [Christensen and Lay, 1988]. Scholz and Small [1997] use these earthquakes and corresponding subducting features in the context of their model of seamount subduction, suggesting increases in normal stress and local seismic coupling in the areas where large bathymetric features are subducted.

Peru-Chile

Along the Peru-Chile margin, several large features, such as Nazca and Carnegie Ridges, are subducted. The 1996 M_w 8.0 Peru earthquake occurred in the region of the subducting Nazca Ridge. The earthquake source model produced by Spence *et al.* [1999] shows patches of high slip collocated with ridge subduction, as well as high slip to the southeastern side of the projected subducted ridge (fig. 5.3). Spence *et al.* [1999] suggest that the subducted ridge provides increased coupling in this region and that the 1942 $M_w \sim 8$ earthquake was also likely related to the subduction of the Nazca Ridge. Gutscher *et al.* [1999] uses a large historical earthquake database in conjunction with detailed bathymetry data and projections of continued ridge subduction to suggest the Carnegie Ridge significantly affects seismic coupling. They find unlike the Nazca Ridge, great earthquakes occur on the flanks of the subducted ridge, not within the ridge-upper plate contact area.

Nankai

Using detailed bathymetric and seismic data, Park *et al.* [1999] and Kodaira *et al.* [2000, 2003] have imaged seamounts and ridges impacting the Nankai subduc-

tion zone (fig. 5.3). Observations of a subducting seamount in the rupture area of the great 1946 Nankaido earthquake have been related to seismic coupling variations. Analysis using seismic data suggests a smaller rupture area than geodetic data analysis, with the westernmost edge of the seismic area estimate abutting the subducted seamount [Kodaira *et al.*, 2000]. Geodetic estimates suggest additional rupture to the southwest of this seamount, leading to the idea that the subducted seamount increased local coupling enough to stop seismogenic rupture propagation to the southwest; however, slow slip was accommodated on an accretionary wedge splay fault southwest of the subducted seamount [Kato and Ando, 1997; Kodaira *et al.*, 2000]. To the east of the 1946 earthquake slip region, seismic reflection data show a feature at depth similar in size and likely origin to the present-day Zenisu Ridge. This subducted ridge is located in the area of rupture termination for the great 1944 Tonankai earthquake [Kodaira *et al.*, 2003]. Given the correlation between subducted feature locations and rupture termination for great earthquakes in this subduction zone, many have suggested that these features act as barriers rather than rupture asperities at least in these earthquakes [Kodaira *et al.*, 2000; 2003]. It is unknown whether their role will change over several earthquake cycles.

Costa Rica

Along the Middle America Trench offshore Costa Rica, detailed bathymetry data show considerable diversity in high-relief features on the subducting Cocos plate. Large earthquakes have occurred along this complex margin and show evidence for rupture diversity that has been linked to the diverse subducting features. Because of the quality of data and ability to show connections between several earthquakes and subducting features, the next few sections detail the structures and seismicity of this region.

Costa Rica Tectonic Structures The Cocos plate offshore Costa Rica can be divided into several domains on the basis of morphologic features, as seen in detailed bathymetry data from Ranero *et al.* [2003] (fig. 5.4). Near the Nicoya Peninsula, the oceanic crust is smooth with a 500 m thick sediment blanket covering the plate [von Huene *et al.*, 2000]. Offshore central Costa Rica, between the Nicoya and Osa peninsulas, the seafloor is disrupted by the Quepos Plateau and many seamounts. Approximately 40% of the oceanic crust offshore central Costa Rica is covered by seamounts that range in size between 1–2.5 km high and 10–20 km wide [Ranero and von Huene, 2000]. The ~200–300 km wide Cocos Ridge, an area of thickened oceanic crust and elevated seafloor [Walther, 2003; Kolarsky *et al.*, 1995], subducts to the southeast offshore the Osa Peninsula. This highly heterogeneous feature is likely a trace of the Galapagos hot spot as the Cocos plate passed over the hot spot during the Miocene [Barckhausen *et al.*, 2001]. These features create diversity in the overriding plate deformation with increased local relief in regions where these features are subducting [Gardner

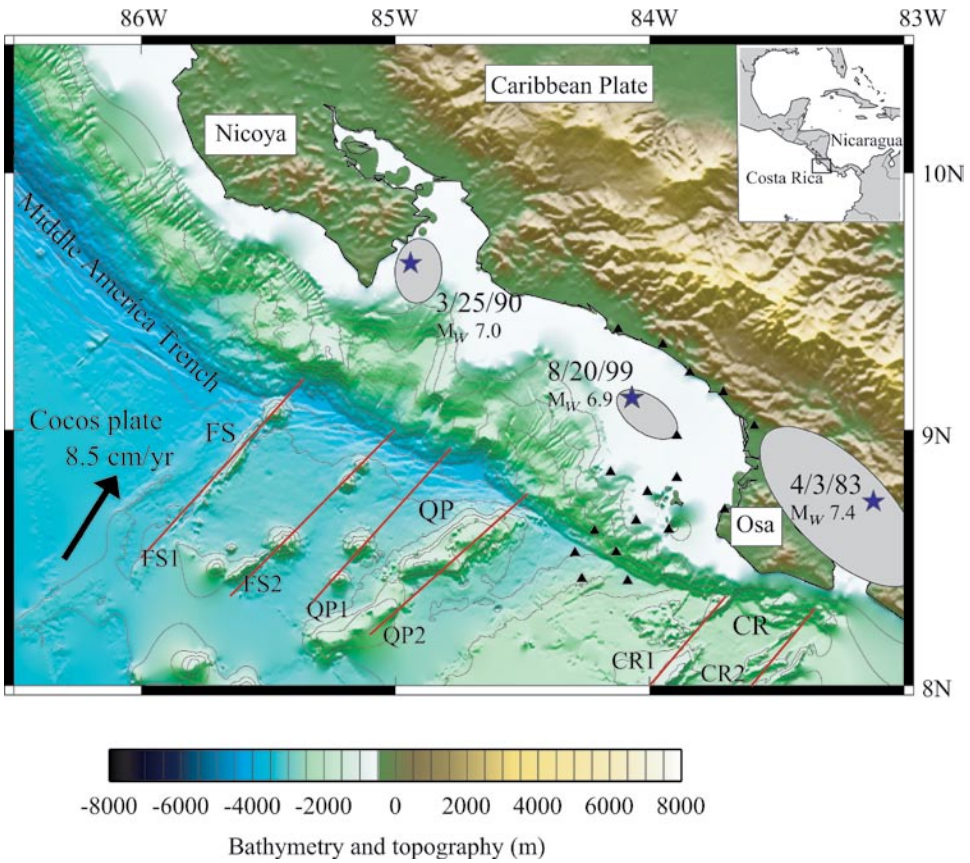


Figure 5.4 Bathymetric features and seismicity in the Middle America Trench offshore Costa Rica. Bathymetry data are from *Ranero et al.* [2003]. There is significant diversity in the subducting Cocos plate features, with the Fisher seamounts (FS), Quepos Plateau (QP), and Cocos Ridge (CR) subducting along this part of the margin. Large earthquakes in 1990, 1999, and 1983 (gray shaded areas show rupture areas for each earthquake) have occurred downdip of these subducting features. Figure 5.6 compares source time functions and rupture areas of these earthquakes with the size of subducting features, with feature size estimated in cross-section profiles (along the red lines).

et al., 1992; *von Huene et al.*, 1995; *Fisher et al.*, 1998; *Dominquez et al.*, 1998; *von Huene et al.*, 2000].

Relationship to Costa Rica Earthquakes These subducting features have been correlated with large historical earthquakes along the margin. *Protti et al.* [1995a] note that the largest underthrusting earthquakes with magnitude ≥ 7.5 have historically occurred only along the Nicoya Peninsula, where they infer the smooth subducted seafloor creates strong seismic coupling to act as a sin-

gle large asperity. However, GPS data from *Norabuena et al.* [2004] show a more patchy distribution of locking. Other large thrust events (M_s up to 7.4) occur in southern Costa Rica where subduction of the buoyant Cocos Ridge creates moderate plate coupling. Earthquakes with maximum magnitudes of only $M < 7.0$ characterize the central Costa Rica region where isolated seamounts are subducted. *von Huene et al.* [2000] suggest that seamounts associated with the Fisher Seamount Chain near the southern tip of Nicoya are related to large earthquakes ($M_s = 6.4\text{--}7.0$) in the region. As there is no evidence for sheared off seamounts along the slope region, *von Huene et al.* [2000] propose that the seamounts enter the seismogenic zone and act as asperities for future earthquakes. Shallow, smaller-magnitude seismicity is more common in regions of seamount and disrupted crust subduction than in the smoother region subducting off northern Costa Rica.

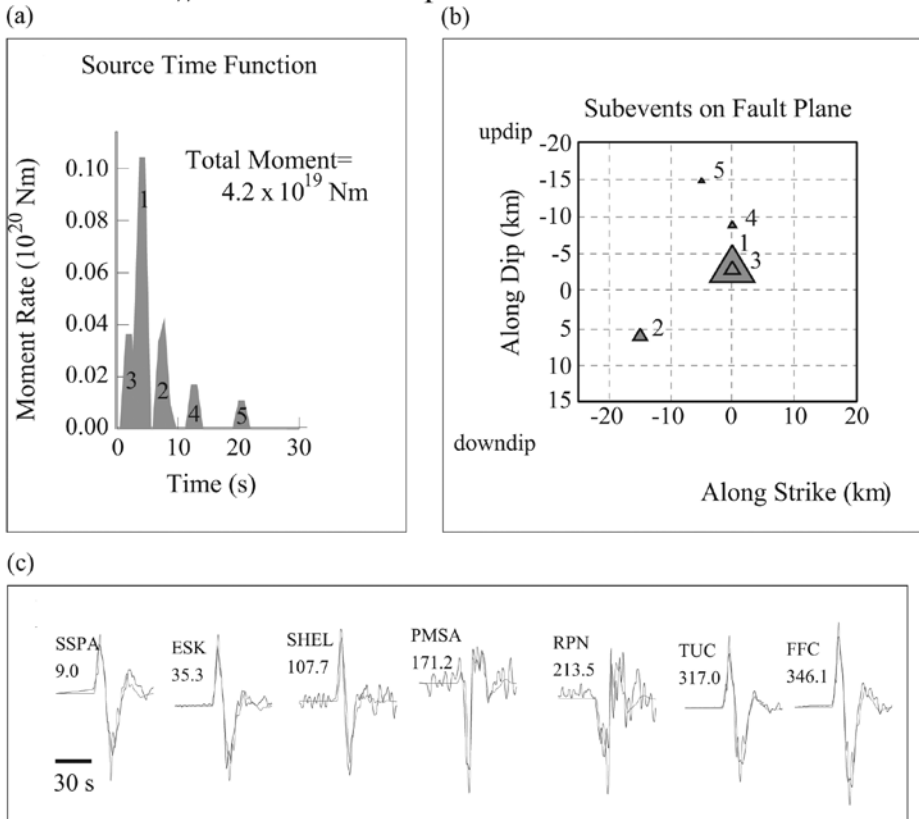
During the 1980s and 1990s, three large ($M_w \geq 6.9$) earthquakes occurred within the different morphological domains in central Costa Rica (fig. 5.4). These earthquakes, well recorded with modern seismic instruments, provide an opportunity to go beyond correlating only the locations of large earthquakes and seafloor features to also examining possible influence of variable seafloor topography on earthquake rupture behavior. The $M_w = 6.9$ underthrusting earthquake in 1999 occurred northwest of the Osa Peninsula in the area of seamount and Quepos Plateau subduction. The other earthquakes occurred in the vicinity of the Fisher Seamount Chain (1990 $M_w = 7.0$) and near the Osa Peninsula and Cocos Ridge (1983 $M_w = 7.4$).

Source time functions for these earthquakes show variations in moment release patterns. For the 1999 Quepos earthquake, *Bilek et al.* [2003] use a variety of methods and data sets, producing consistent source models using both surface- and body-wave inversions. Most of the seismic moment was released in one main event (event 1), with minor moment release occurring in later, smaller subevents within the first 10 s, as shown in the source time function in figure 5.5. The time function overall is very simple, suggesting a simple rupture for this earthquake. Figure 5.5 also shows the locations of the subevents on the fault plane; the moment was concentrated spatially, with some rupture propagating to the southeast with a direction of $\sim 100^\circ$ (going from subevent 1 to subevent 2).

The 1990 $M_w = 7.0$ Nicoya Gulf earthquake had slightly more complexity in the rupture history compared to the 1999 Quepos earthquake. *Protti et al.* [1995b] describe two large subevents of moment release between 18 and 24 km depth (fig. 5.6). Aftershock patterns suggest an initial rupture area of $\leq 600 \text{ km}^2$ [*Protti et al.*, 1995b].

The 1983 Osa earthquake ($M_w = 7.4$) was one of the largest underthrusting earthquakes to occur in the Osa Peninsula region, with others occurring in 1904 ($M_s = 7.6$) and 1941 ($M_s = 7.5$) [*Tajima and Kikuchi*, 1995]. Body-wave analyses of the 1983 earthquake consistently show a more complicated rupture process than either the 1990 and 1999 events with longer source duration, more

1999 M_W 6.9 Osa Earthquake

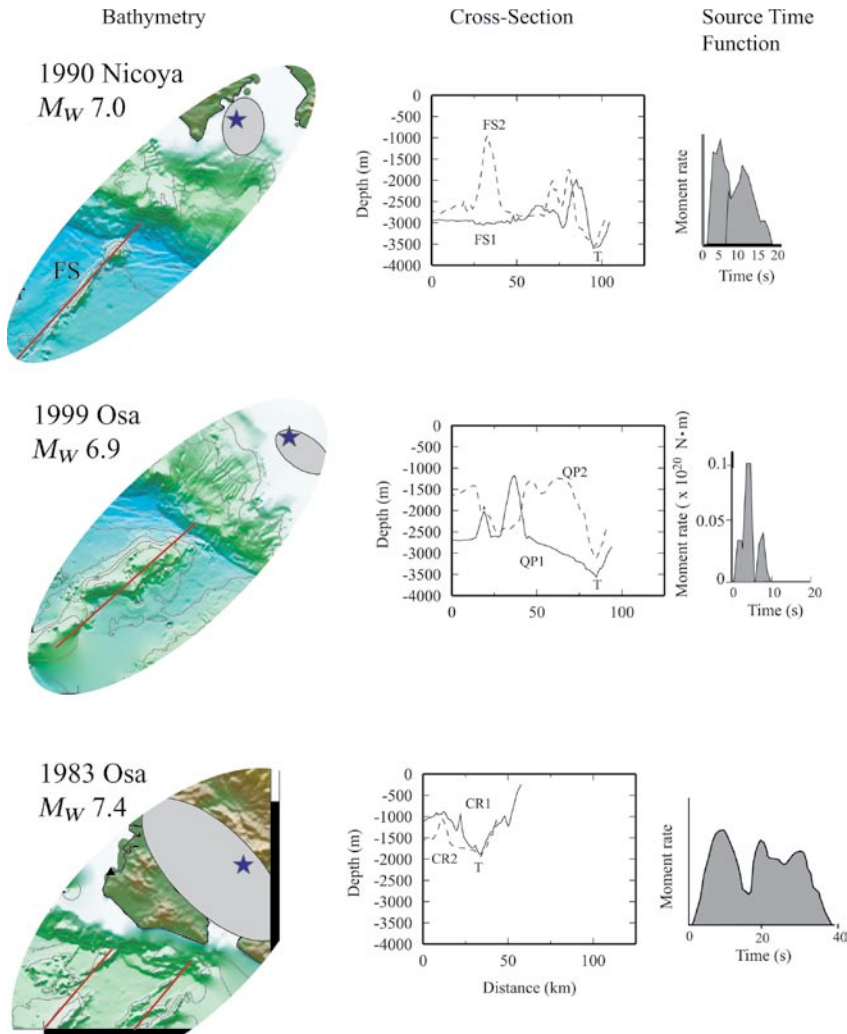


AU: In fig. 5.5, you write “1999 Mw 6.9 Osa Earthquake”, but in the caption, you write “1999 Quepos earthquake”; which is correct?

Figure 5.5 Determination of source time function and locations of main moment release for the 1999 Quepos earthquake, modified from *Bilek et al.* [2003]. This analysis involved inverting body-wave seismograms to find the best spatial and temporal distribution of moment release using the method of *Kikuchi and Kanamori* [1986]. (a) The source time function shows the majority of moment release occurred in the first large pulse, with minor moment release in pulses 2 and 3, during 10 s of rupture. (b) Pulses of moment release seen in the source time function are located on the two-dimensional (2-D) fault plane, oriented along strike (313°). The main pulses of moment release are fairly concentrated spatially, with minor rupture toward the southeast (going from 1 to 2). (c) Representative seismograms (black) used in the inversion, with station name and azimuth from the earthquake listed, as well as the predicted seismograms (red) for the best inversion model.

complexity in the source time function, and possible mechanism variations along strike [*Adamek et al.*, 1987; *Tajima and Kikuchi*, 1995].

Bathymetric data offshore Costa Rica allow for comparisons between bathymetric feature size with rupture areas of these large earthquakes (fig. 5.6). Cross sections through these features provide estimates of feature size that are com-



AU: In fig. 5.6, you write “1999 Osa Mw 6.9”, but in the caption, you write “1999 Quepos earthquake”; which is correct? And for the 1983 Osa (see bottom of fig. 5.6)?

Figure 5.6 Comparison of Costa Rica earthquake rupture details with subducting features. For the 1990 Nicoya earthquake, two main pulses of moment release in the source time function suggest the rupture of 2 closely spaced asperities. Early aftershock patterns suggest a rupture area of $\sim 600 \text{ km}^2$. Seamounts in the Fisher Seamount Group range in size between ~ 300 and 400 km^2 . As the earthquake source details are comparable to the sizes of the subducting seamounts, *Protti et al.* [1995b] and *Bilek et al.* [2003] suggest that the 1990 earthquake was the rupture of seamount contacts with the upper plate. The 1999 Quepos earthquake had 1–2 main pulses of moment release in the source time function and an aftershock region of $\sim 400 \text{ km}^2$, which can be explained by rupture of a portion of the Quepos Plateau [*Bilek et al.*, 2003]. The source time function for the 1983 earthquake contains more complexity than either the 1990 or 1999 events. On the basis of its location and rupture details from *Tajima and Kikuchi* [1995], this earthquake ruptured much of the along-strike extent of the Cocos Ridge, likely causing the complexity seen in the rupture process.

parable to the size of earthquake rupture area. Projecting the Quepos Plateau section of subducting crust along the plate motion vector intersects the location of the 1999 Quepos earthquake, suggesting that the earthquake slip may represent the rupture of specific plateau contact zones with the overriding plate. This scenario can explain the concentrated and simple nature of moment release for this earthquake. Figure 5.6 shows two cross sections through the Quepos Plateau area (QP1 and QP2 lines in fig. 5.4). Several of the subducting features in this region have dimensions of 12–25 km along the dip direction (as represented in the cross section across one of these features) and comparable dimensions in the strike dimension (150–400 km² in area), including several high patches of the Quepos Plateau and large seamounts to the northwest of the Quepos Plateau. The aftershock region (~400 km²) does not extend beyond the along-strike width of the Quepos Plateau (fig. 5.7). *Bilek et al.* [2003] and *DeShon et al.* [2003] suggest that the Quepos Plateau served as the rupture asperity for the 1999 earthquake.

In the region of the 1990 Nicoya Gulf earthquake, the Fisher seamounts are clearly seen in the bathymetry data and are subducting at the southern end of the Nicoya Peninsula, seaward of the location of the 1990 earthquake. Individual seamounts within the chain can reach ~300–400 km², while small seamount pairs have composite area of ~200–250 km² [*von Huene et al.*, 2000]. On the basis of the bathymetry data and the rupture process determined for this event, *Protti et al.* [1995b] suggest that the 1990 earthquake represents the rupture of seamount contacts with the overriding plate. Rupture of more than one seamount within the seamount chain could produce the separate subevents of moment release determined for the 1990 Nicoya Gulf event.

Additional support for subducted seamounts at depth in the region comes from regional geology as well as seismic tomography images produced for this region. Seamounts at depth would likely produce some fore-arc uplift. *Marshall and Anderson* [1995] and *Gardner et al.* [2001] use radiocarbon dating of terraces and rotation in southeastern Nicoya to estimate ~400 km² of uplift at the tip of the peninsula. *Husen et al.* [2002] use data from over 3700 earthquakes to tomographically image a thick feature on the slab at approximately the same location and depth of the 1990 earthquake. They suggest the imaged feature is the subducted seamount that served as the asperity for the 1990 earthquake rupture.

The complex 1983 earthquake occurred to the southeast near the highly disturbed crust containing the Cocos Ridge. The broad arch of the ridge has topography of ~1 km high where it enters the Middle America Trench with variable sediment thickness along the ridge [*von Huene et al.*, 2000; *Walther*, 2003]. Comparing the locations of moment release obtained by *Tajima and Kikuchi* [1995] with regional bathymetry in the south suggests that this earthquake ruptured both of the elevated features (between CR1 and CR2) on the high area of the Cocos Ridge along with additional rupture propagation to the SE (fig. 5.4). The high subducted relief and sediment thickness in the area of

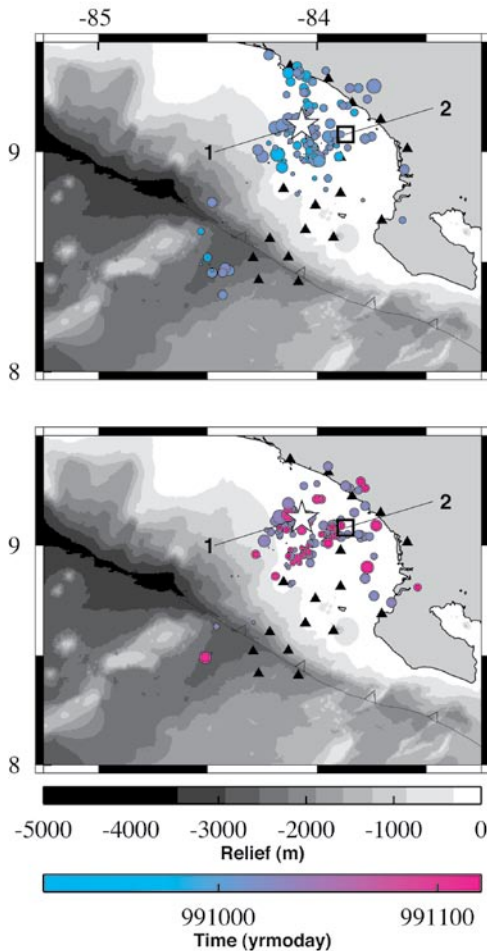


Figure 5.7 Aftershocks for the 1999 Quepos earthquake as recorded by a temporary onshore-offshore seismic network (triangles) [DeShon *et al.*, 2003]. The large star and box indicate the locations of the main two subevents of moment release for the 1999 event. Small circles are aftershock locations, colored by time after the main earthquake. The top panel shows that the earliest (first 2 months) aftershocks are spread between the areas of main moment release but do not extend much beyond the projected lateral extent of the Quepos Plateau. The bottom panel shows the final month of aftershock recording, when seismicity appears to be mainly located on what may be the flanks of the previously subducted Quepos Ridge.

the 1983 rupture led to the more complicated rupture behavior of this event (fig. 5.6) [Bilek *et al.*, 2003]. On the basis of these correlations between earthquake patterns and subducted features, it seems likely that earthquake magnitudes along the Costa Rica margin may be controlled by feature size, an important consideration for hazard assessments.

Discussion

Temporal Variability of Asperities

An important question connected with determining the physical or geologic nature of asperities is that of consistency of these features over several earthquake cycles. Some evidence suggests that these features are consistent over

at least relatively short timescales. For instance, GPS data in a few subduction zones suggest that rupture zone patches of high slip during past large earthquakes currently accumulate more strain than adjacent regions that did not produce high slip. This appears to be the case for central and southern Japan [Sagiya, 1999; Sagiya *et al.*, 2000] as well as in the region of the 1964 great Alaska earthquake [Freymueller *et al.*, 2000, Zweck *et al.*, 2002]. In Costa Rica, part of the rupture area of the 1950 M 7.7 earthquake is also locked and accumulating strain at close to the plate rate [Norabuena *et al.*, 2004].

Seismic data collected offshore NE Japan also suggest temporal stability of asperities as defined by small earthquakes. Using 8 years of data, Matsuzawa *et al.* [2002] and Igarashi *et al.* [2003] locate several clusters of repeating small magnitude ($M \sim 4.8$) earthquakes with similar focal mechanisms along the plate boundary. They suggest that these earthquakes are due to repeating slips of small asperities (on the order of 0.1–1 km) surrounded by regions of stable sliding. They find that these small earthquakes are not collocated with regions of high moment release during large earthquakes but in areas surrounding the high moment release zones. This model suggests that several different sized strong regions exist in the region but that the smaller strong regions persist over at least short time periods. Okada *et al.* [2003] compare rupture areas of small earthquakes in NE Japan occurring in 1995 and 2001, finding significant overlap that supports a persistent asperity hypothesis. This would be consistent with repeating small earthquakes and persistent small asperities observed for strike slip faults such as the San Andreas fault [Nadeau and Johnson, 1998].

Using this idea of consistent asperities within the fault zone over some timescale, variations in earthquakes along the western margin of Costa Rica can be used to make assessments of the coupling and earthquake recurrence possibilities for this region. Protti *et al.* [1995a] and Nishenko [1991] segment the margin on the basis of magnitudes of previous earthquakes and inferred seismic coupling. In terms of the earthquakes described in the previous section, the 1999 earthquake is an example of the typical central segment event, whereas the more complicated 1983 earthquake is a typical Osa segment event. Size and location of earthquakes in the Quepos segment are likely limited by the number and size of incoming seamount and Quepos Plateau features, although heterogeneous coupling allows for the rupture of one or two closely spaced seamount features but does not continue beyond these features. The Nicoya and Osa segments experience more frequent large earthquakes because of smoother plate subduction (Nicoya) or continued subduction of the Cocos Ridge (Osa).

However, recurrence of large earthquakes in several subduction zones suggests that temporal persistence of asperities is complicated. Schwartz [1999] compares high-slip regions for recent subduction zone that occurred in regions of past large earthquakes for which slip information is available. In some regions, large earthquake slip for recent events is collocated with high slip in past events (i.e., Kuriles and Aleutian earthquakes). However, high slip for

earthquakes in NE Japan and the Solomon Islands filled areas of low slip in previous earthquakes. This suggests that simple geometric or material variations in the subduction zones may not be solely responsible for controlling slip heterogeneity.

Subducted Features as Asperities and Barriers

Correlations between subducting features and high slip during earthquakes are complicated, as it appears that features can act as either asperities or barriers to rupture (fig. 5.8). Additionally, this behavior may not be consistent over many earthquake cycles, possibly related to variable strength of asperities. Observations from Nankai suggest these features, once subducted, act as barriers to seismic rupture at least through one earthquake cycle [Kodaira *et al.*, 2000]. In Costa Rica, Java, and other areas, it appears that these features are the locations of high earthquake slip. The roles of the subducted seamounts might depend on the degree of seismic coupling in each region such that weakly coupled margins might have seamounts that only act as asperities, while seamounts in strongly coupled margins could act as either. Variations in stresses or friction might allow for the role of seamounts to change over the seismic

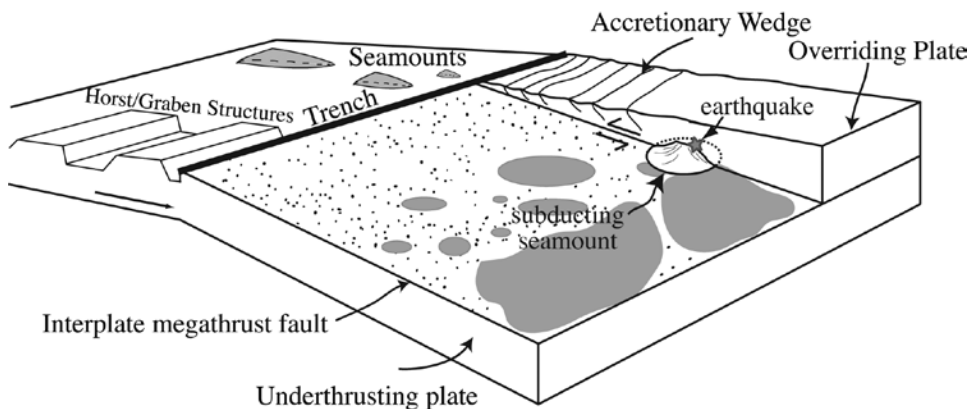


Figure 5.8 Cartoon of the shallow subduction environment. Asperity distribution (gray) may be very heterogeneous at depth based on the diversity of features, such as seamounts, horst, and graben structures, on the incoming plate. Between the asperity or high-strength regions, weaker material (dotted regions) may limit earthquake rupture. This cartoon shows the possibility of a subducted seamount being a location for earthquake rupture, as suggested for Costa Rica, Java, and Alaska. However, other factors may be important, such as the relative strength of the upper plate material and frictional variations on the plate interface. In addition, regions such as Nankai appear to have different behavior, with earthquakes beginning away from but terminating at previously subducted high-relief features.

cycle or several cycles and may impact regions such as Nankai, Costa Rica, and Java. Further identification of subducted features and determination of their roles in regional seismicity is needed to address this question.

Conclusions

Heterogeneous slip is found in earthquakes of all tectonic environments, allowing for these patterns to be broadly defined with models of heterogeneous asperity distribution along faults. As shallow subduction zones produce much of the global seismicity, understanding the nature of the strong patches and heterogeneous slip patterns for subduction-zone earthquakes is an important endeavor as it may provide insight into seismic hazards. The physical nature of the strong patches on subduction-zone megathrust faults may range from fault-friction variations, strength of adjacent fore-arc material, and various structural features on the subducting plate, as correlations have been made between earthquake behavior and all of these possibilities. However, more work is needed in several areas, such as increased mapping of subducting features in all subduction zones, better knowledge of frictional properties of subduction fault zone materials, and understanding of subduction-zone stress patterns, before a complete understanding of the interaction between subduction-zone features and large earthquakes is achieved.

Acknowledgments

Several ideas for this paper resulted from discussions during the 2003 MARGINS SEIZE Theoretical Institute meeting. H. Kanamori and A. Newman provided constructive reviews to improve the manuscript. Earthquake data were obtained from the IRIS Data Management Center. Bathymetry data used for several of the Costa Rica figures were kindly provided by C. Ranero and R. von Huene. GMT software [Wessel and Smith, 1991] was used for some figure preparation. This work was partially supported by a Turner postdoctoral fellowship from the University of Michigan.

References

- Abercrombie, R. E., M. Antolik, K. Felzer, and G. Ekström (2001), The 1994 Java tsunami earthquake: Slip over a subducting seamount, *J. Geophys. Res.*, *106*, 6595–6607.
- Adamek, S., F. Tajima, and D. A. Wiens (1987), Seismic rupture associated with subduction of the Cocos Ridge, *Tectonics*, *6*, 757–774.
- Ammon, C. J., A. A. Velasco, and T. Lay (1993), Rapid estimation of rupture directivity: Application to the 1992 Landers ($M_s = 7.4$) and Cape Mendocino ($M_s = 7.2$) California earthquakes, *Geophys. Res. Lett.*, *20*, 97–100.

- Ando, M. (1975), Source mechanisms and tectonic significance of historical earthquakes along the Nankai Trough, Japan, *Tectonophysics*, 27, 119–140.
- Balance, P. F., D. W. Scholl, T. L. Vallier, and R. H. Herzer (1989), Subduction of a late Cretaceous seamount of the Louisville Ridge at the Tonga Trench: A model of normal and accelerated tectonic erosion, *Tectonics*, 8, 853–962.
- Barckhausen, U., C. R. Ranero, R. von Huene, S. C. Cande, and H. A. Roeser (2001), Revised tectonic boundaries in the Cocos Plate off Costa Rica: Implications for the segmentation of the convergent margin and for plate tectonic models, *J. Geophys. Res.*, 106, 19, 207–19,220.
- Beck, S. L., and D. H. Christensen (1991), Rupture process of the February 4, 1965 Rat Islands earthquake, *J. Geophys. Res.*, 96, 2205–2221.
- Beroza, G. C. (1991), Near-source modeling of the Loma Prieta earthquake: Evidence for heterogeneous slip and implications for earthquake hazard, *Bull. Seismol. Soc. Am.*, 81, 1603–1621.
- Bilek, S. L., S. Y. Schwartz, and H. R. DeShon (2003), Control of seafloor roughness on earthquake rupture behavior, *Geology*, 31(5), 455–458.
- Byerlee, J. D. (1967), Theory of friction based on brittle fracture, *J. Appl. Phys.*, 38, 2928–2934.
- Chapel, D., and C. Small (1996), Distribution of large seamounts in the Pacific Ocean, *Eos Trans. AGU*, 77, Fall Meet. Suppl., F770.
- Christensen, D., and T. Lay (1988), Large earthquakes in the Tonga region associated with subduction of the Louisville Ridge, *J. Geophys. Res.*, 93, 13,367–13,389.
- Cloos, M. (1992), Thrust-type subduction zone earthquakes and seamount asperities: A physical model for seismic rupture, *Geology*, 20(7), 601–604.
- Cloos, M., and R. L. Shreve (1996), Shear-zone thickness and the seismicity of Chilean- and Marianas-type subduction zones, *Geology*, 24(2), 107–110.
- DeShon, H. R., S. Y. Schwartz, S. L. Bilek, L. M. Dorman, V. Gonzalez, J. M. Protti, E. R. Flueh, and T. H. Dixon (2003), Seismogenic zone structure off the southern Middle America Trench, Costa Rica, *J. Geophys. Res.*, 108(B10), 2491, doi:10.1029/2002JB002294.
- Dominquez, S., S. E. Lallemand, J. Malavieille, and R. von Huene (1998), Upper plate deformation associated with seamount subduction, *Tectonophysics*, 293, 207–224.
- Estabrook, C. H., K. H. Jacob, and L. R. Sykes (1994), Body wave and surface wave analysis of large and great earthquakes along the eastern Aleutian Arc, 1923–1993: Implications for future events, *J. Geophys. Res.*, 99, 11,643–11,662.
- Fisher, D. M., T. W. Gardner, J. S. Marshall, P. B. Sak, and M. Protti (1998), Effect of subducting sea-floor roughness on fore-arc kinematics, Pacific coast, Costa Rica, *Geology*, 26(5), 467–470.
- Freymueller, J. T., S. C. Cohen, and H. J. Fletcher (2000), Spatial variations in present-day deformation, Kenai Peninsula, Alaska, and their implications, *J. Geophys. Res.*, 105, 8079–8101.
- Gardner, T. W., D. Verdonck, N. M. Pinter, R. Slingerland, K. P. Furlong, T. F. Bullard, and S. G. Wells (1992), Quaternary uplift astride the aseismic Cocos Ridge, Pacific coast, Costa Rica, *Geol. Soc. Am. Bull.*, 104, 219–232.
- Gardner, T. W., J. Marshall, D. Merritts, B. Bee, R. Burgette, E. Burton, J. Cooke, N. Kehrwald, M. Protti, D. Fisher, and P. Sak (2001), Holocene forearc block rotation in response to seamount subduction, southeastern Peninsula de Nicoya, Costa Rica, *Geology*, 29(2), 151–154.
- Gutscher, M.-A., J. Malavieille, S. Lallemand, and J.-Y. Collot (1999), Tectonic segmentation of the North Andean margin: Impact of the Carnegie Ridge collision, *Earth Planet. Sci. Lett.*, 168, 255–270.
- Heaton, T. H. (1990), Evidence for and implications of self-healing pulses of slip in earthquake rupture, *Phys. Earth Planet. Inter.*, 64, 1–20.
- Hilde, T. W. C. (1983), Sediment subduction vs. accretion around the Pacific, *Tectonophysics*, 99, 381–397.

- Hino, R., T. Kanazawa, and A. Hasegawa (1996), Interplate seismic activity near the northern Japan Trench deduced from ocean bottom and land-based seismic observations, *Phys. Earth Planet. Inter.*, 93, 37–52.
- Husen, S., E. Kissling, and R. Quintero (2002), Tomographic evidence for a subducted seamount beneath the Gulf of Nicoya, Costa Rica: The cause of the 1990 $M_w = 7.0$ Gulf of Nicoya earthquake, *Geophys. Res. Lett.*, 29(8), 1238, doi:10.1029/2001GL014045.
- Igarashi, T., T. Matsuzawa, and A. Hasegawa (2003), Repeating earthquakes and interplate aseismic slip in the northeastern Japan subduction zone, *J. Geophys. Res.*, 108(B5), 2249, doi:10.1029/2002JB001920.
- Ji, C., D. J. Wald, and D. V. Helmberger (2002), Source description of the 1999 Hector Mine, California, earthquake, part II: Complexity of slip history, *Bull. Seismol. Soc. Am.*, 92, 1208–1226.
- Kanamori, H. (1978), Use of seismic radiation to infer source parameters, *U.S. Geol. Surv. Open File Rep.*, 380, 283–318.
- Kanamori, H. (1986), Rupture process of subduction-zone earthquakes, *Annu. Rev. Earth Planet. Sci.*, 14, 293–322.
- Kato, T., and M. Ando (1997), Source mechanisms of the 1944 Tonankai and 1946 Nankaido earthquakes: Spatial heterogeneity of rise times, *Geophys. Res. Lett.*, 24, 2055–2058.
- Kelleher, J., and W. McCann (1976), Buoyant zones, great earthquakes, and unstable boundaries of subduction, *J. Geophys. Res.*, 81, 4885–4896.
- Kelleher, J., and W. McCann (1977), Bathymetric highs and the development of convergent plate boundaries, in *Island Arcs, Deep Sea Trenchs, and Back-Arc Basins, Maurice Ewing Ser.*, vol. 1, edited by M. Talwani and W. C. Pitman, pp. 115–122, AGU, Washington, D. C.
- Kikuchi, M., and H. Kanamori (1986), Inversion of complex body waves—II, *Phys. Earth Planet. Int.*, 43, 205–222.
- Kodaira, S., N. Takahashi, A. Nakanishi, S. Miura, and Y. Kaneda (2000), Subducted seamount imaged in the rupture zone of the 1946 Nankaido earthquake, *Science*, 289, 104–106.
- Kodaira, S., A. Nakanishi, J.-O. Park, A. Ito, T. Tsuru, and Y. Kaneda (2003), Cyclic ridge subduction at an inter-plate locked zone off central Japan, *Geophys. Res. Lett.*, 30(6), 1339, doi:10.1029/2002GL016595.
- Kolarsky, R. A., P. Mann, and W. Montero (1995), Island arc response to shallow subduction of the Cocos Ridge, Costa Rica, in *Geologic and Tectonic Development of the Caribbean Plate Boundary in Southern Central America*, edited by P. Mann, *Geol. Soc. Am. Spec. Pap.*, 295, 235–262.
- Lallemand, S., and X. Le Pinchon (1987), Coulomb wedge model applied to subduction of seamounts in the Japan Trench, *Geology*, 15, 1065–1069.
- Lallemand, S., R. Culotta, and R. von Huene (1989), Subduction of the Daiichi Kashima seamount in the Japan Trench, *Tectonophysics*, 160, 231–247.
- Lay, T., and H. Kanamori (1980), Earthquake doublets in the Solomon Islands, *Phys. Earth Planet. Int.*, 21, 283–304.
- Lay, T., H. Kanamori, and L. Ruff (1982), The asperity model and the nature of large subduction zone earthquakes, *Earthquake Predict. Res.*, 1, 3–71.
- Ma, K.-F., J. Mori, S.-J. Lee, and S. B. Yu (2001), Spatial and temporal distribution of slip for the 1999 Chi-Chi, Taiwan, earthquake, *Bull. Seismol. Soc. Am.*, 91, 1069–1087.
- Marshall, J., and R. Anderson (1995), Quaternary uplift and seismic cycle deformation, Peninsula de Nicoya, Costa Rica, *Geol. Soc. Am. Bull.*, 107, 463–473.
- Masson, D. G., L. M. Parson, J. Milsom, G. Nichols, N. Sikumbang, B. Dwiyanto, and H. Kallagher (1990), Subduction of seamounts at the Java Trench: A view with long-range sidescan sonar, *Tectonophysics*, 185, 51–65.
- Matsuzawa, T., T. Igarashi, and A. Hasegawa (2002), Characteristic small-earthquake sequence off Sanriku, northeastern Honshu, Japan, *Geophys. Res. Lett.*, 29(11), 1543, doi:10.1029/2001GL014632.

- McCaffrey, R. (1993), On the role of the upper plate in great subduction zone earthquakes, *J. Geophys. Res.*, *98*, 11,953–11,966.
- McCaffrey, R. (1994), Global variability in subduction thrust fore-arc systems, *Pure Appl. Geophys.*, *142*, 173–224.
- Mendoza, C., and S. H. Hartzell (1988), Inversion for slip distribution using GDSN P waves: North Palm Springs, Borah Peak, and Michoacan earthquakes, *Bull. Seismol. Soc. Am.*, *78*, 1092–1111.
- Nadeau, R. M., and L. R. Johnson (1998), Seismological studies at Parkfield VI: Moment release rates and estimates of source parameters for small repeating earthquakes, *Bull. Seismol. Soc. Am.*, *88*, 790–814.
- Nishenko, S. P. (1991), Circum-Pacific seismic potential: 1989–1999, *Pure Appl. Geophys.*, *135*, 169–259.
- Norabuena, E., et al. (2004), Geodetic and seismic constraints on some seismogenic zone processes in Costa Rica, *J. Geophys. Res.*, *109*, B11403, doi:10.1029/2003JB002931.
- Obana, K., S. Kodaira, Y. Kaneda, K. Mochizuki, M. Shinohara, and K. Suyehiro (2003), Microseismicity at the seaward updip limit of the western Nankai Trough seismogenic zone, *J. Geophys. Res.*, *108*(B10), 2459, doi:10.1029/2002JB002370.
- Okada, T., T. Matsuzawa, and A. Hasegawa (2003), Comparison of source areas of $M_{4.8} \pm 0.1$ repeating earthquakes off Kamaishi, NE Japan: Are asperities persistent features?, *Earth Plant. Sci. Lett.*, *213*, 361–374.
- Pacheco, J. F., and L. R. Sykes (1992), Seismic moment catalog of large, shallow earthquakes, 1900–1989, *Bull. Seismol. Soc. Am.*, *82*, 1306–1349.
- Park, J.-O., T. Tsuru, Y. Kaneda, Y. Kono, S. Kodaira, N. Takahashi, and H. Kinoshita (1999), A subducting seamount beneath the Nankai accretionary prism off Shikoku, southwestern Japan, *Geophys. Res. Lett.*, *26*, 931–934.
- Protti, M., F. Güendel, and K. McNally (1995a), Correlation between the age of the subducting Cocos plate and the geometry of the Wadati-Benioff zone under Nicaragua and Costa Rica, in *Geologic and Tectonic Development of the Caribbean Plate Boundary in Southern Central America*, edited by P. Mann, *Spec. Pap. Geol. Soc. Am.*, *295*, 309–326.
- Protti, M., et al. (1995b), The March 25, 1990 ($M_w = 7.0$, $M_L = 6.8$) earthquake at the entrance of the Nicoya Gulf, Costa Rica: Its prior activity, foreshocks, aftershocks, and triggered seismicity, *J. Geophys. Res.*, *100*, 20,345–20,358.
- Ranero, C. R., and R von Huene (2000), Subduction erosion along the Middle America convergent margin, *Nature*, *404*, 748–752.
- Ranero, C. R., J. Phipps Morgan, K. McIntosh, and C. Reichert (2003), Bending-related faulting and mantle serpentinitization at the Middle America Trench, *Nature*, *425*, 367–373.
- Rice, J. R. (1993), Spatiotemporal complexity of slip on a fault, *J. Geophys. Res.*, *98*, 9885–9907.
- Ruff, L. J. (1989), Do trench sediments affect great earthquake occurrence in subduction zones? *Pure Appl. Geophys.*, *129*, 263–282.
- Ruff, L. J. (1992), Asperity distributions and large earthquake occurrence in subduction zones, *Tectonophysics*, *211*, 61–83.
- Ruff, L. J., and H. Kanamori (1980), Seismicity and the subduction process, *Phys. Earth Planet. Int.*, *23*, 240–252.
- Ruff, L. J., and H. Kanamori (1983), The rupture process and asperity distribution of three great earthquakes from long period diffracted *P*-waves, *Phys. Earth Planet. Inter.*, *31*, 202–230.
- Ryan, H. F., and D. W. Scholl (1993), Geologic implications of great interplate earthquakes along the Aleutian arc, *J. Geophys. Res.*, *98*, 22,135–22,146.
- Sagiya, T. (1999), Interplate coupling in the Tokai District, central Japan, deduced by continuous GPS data, *Geophys. Res. Lett.*, *26*, 2315–2318.
- Sagiya, T., S. Miyazaki, and T. Tada (2000), Continuous GPS array and present day crustal deformation of Japan, *Pure Appl. Geophys.*, *157*, 2303–2322.

- Sammis, C. G., and J. R. Rice (2001), Repeating earthquakes as low-stress-drop events at a border between locked and creeping fault patches, *Bull. Seismol. Soc. Am.*, 91, 532–537.
- Scholz, C. H., and J. T. Engelder (1976), The role of asperity indentation and plough in rock friction 1. Asperity creep and stick slip, *Int. J. Rock Mech. Min. Sci. Geomech. Abstr.*, 13, 149–154.
- Scholz, C. H., and C. Small (1997), The effect of seamount subduction on seismic coupling, *Geology*, 25(6), 487–490.
- Schwartz, S. Y. (1999), Noncharacteristic behavior and complex recurrence of large subduction zone earthquakes, *J. Geophys. Res.*, 104, 23,111–23,125.
- Schwartz, S. Y., and L. J. Ruff (1987), Asperity distribution and earthquake occurrence in the southern Kurile Islands arc, *Phys. Earth Planet. Inter.*, 49, 54–77.
- Song, T.-R., and M. Simons (2003), Large trench-parallel gravity variations predict seismogenic behavior in subduction zones, *Science*, 301, 630–633.
- Spence, W., C. Mendoza, E. R. Engdahl, G. L. Choy, and E. Norabuena (1999), Seismic subduction of the Nazca Ridge as shown by the 1996–1997 Peru earthquake, *Pure Appl. Geophys.* 154, 753–776.
- Tajima, F., and M. Kikuchi (1995), Tectonic implications of the seismic ruptures associated with the 1983 and 1991 Costa Rica earthquakes, in *Geologic and Tectonic Development of the Caribbean Plate Boundary in Southern Central America*, edited by P. Mann, *Spec. Pap. Geol. Soc. Am.*, 295, 327–340.
- Tanioka, Y., L. Ruff, and K. Satake (1997), What controls the lateral variation of large earthquake occurrence along the Japan Trench? *Island Arc*, 6, 261–266.
- Trifunac, M. D., and J. N. Brune (1970), Complexity of energy release during the Imperial Valley, California earthquake of 1940, *Bull. Seismol. Soc. Am.*, 60, 137–160.
- von Huene, R., et al. (1995), Morphotectonics of the Pacific convergent margin of Costa Rica, in *Geologic and Tectonic Development of the Caribbean Plate Boundary in Southern Central America*, edited by P. Mann, *Spec. Pap. Geol. Soc. Am.*, 295, 291–307.
- von Huene, R., C. R. Ranero, and W. Weinrebe (2000), Quaternary convergent margin tectonics of Costa Rica, segmentation of the Cocos Plate, and Central American volcanism, *Tectonics*, 19, 314–334.
- Wald, D. J., and T. H. Heaton (1994), Spatial and temporal distribution of slip for the 1992 Landers, California earthquake, *Bull. Seismol. Soc. Am.*, 84, 668–691.
- Wald, D. J., D. V. Helmberger, and T. H. Heaton (1991), Rupture model of the 1989 Loma Prieta earthquake from the inversion of strong motion and broadband teleseismic data, *Bull. Seismol. Soc. Am.*, 81, 1540–1572.
- Walther, C. H. E. (2003), The crustal structure of Cocos Ridge off Costa Rica, *J. Geophys. Res.*, 108(B3), 2136, doi:10.1029/2001JB000888.
- Wessel, P., and W. H. F. Smith (1991), Free software helps map and display data, *Eos Trans. AGU*, 72, 441–445.
- Wyss, M., and J. N. Brune (1967), The Alaska earthquake of 28 March 1964: A complex multiple source rupture, *Bull. Seismol. Soc. Am.*, 57, 1017–1023.
- Xu, Z. Y., and S. Y. Schwartz (1993), Large earthquake doublets and fault plane heterogeneity in the northern Solomon-Islands subduction zone, *Pure Appl. Geophys.*, 140, 365–390.
- Zweck, C., J. T. Freymueller, and S. C. Cohen (2002), Three-dimensional elastic dislocation model of the post-seismic response to the 1964 Alaska earthquake, *J. Geophys. Res.*, 107(B4), 2064, doi:10.1029/2001JB000409.